Journal of Chromatography A, 1228 (2012) 110–124

Contents lists available at ScienceDirect

Journal of Chromatography A

journal homepage: www.elsevier.com/locate/chroma

# Silica-based, hyper-crosslinked acid stable stationary phases for high performance liquid chromatography

Yu Zhang, Hao Luo, Peter W. Carr*

*Department of Chemistry, University of Minnesota, 207 Pleasant St. S.E., Minneapolis, MN 55455, USA*

ARTICLE INFO

*Article history:*
Available online 6 August 2011

*Keywords:*
Acid stable
High temperature
RPLC
Hyper-crosslinked
Stationary phase
Selectivity

ABSTRACT

A new family of hyper-crosslinked (HC) phases for use under very aggressive acid conditions including those encountered in ultra-fast, high temperature two-dimensional liquid chromatography (2DLC) has been recently introduced. This type of stationary phase shows significantly enhanced acid and thermal stability compared to the most acid stable, commercial RPLC phases. In addition, the use of "orthogonal" chemistry to make surface-confined polymer networks ensures good reproducibility and high efficiency. One of the most interesting features of the HC phases is the ability to derivatize the surface aromatic groups with various functional groups. This has led to the development of a family of hyper-crosslinked phases possessing a wide variety of chromatographic selectivities by attaching hydrophobic (e.g. $-C_8$), ionizable (e.g. –COOH, $-SO_3H$), aromatic (e.g. –toluene) or polar (e.g. –OH) species to the aromatic polymer network. HC reversed phases with various degrees of hydrophobicity and mixed-mode HC phases with added strong and weak cation exchange sites have been synthesized, characterized and applied. These silica-based acid-stable HC phases, with their attractive chromatographic properties, should be very useful in the separation of bases or biological analytes in acidic media, especially at elevated temperatures. This work reviews prior research on HC phases and introduces a novel HC phase made by alternative chemistry.

© 2011 Elsevier B.V. All rights reserved.

## 1. Introduction

The ultimate goal of any chromatographic method development and optimization is to separate the species in the sample by achieving acceptable resolution ($R_S$) in a reasonable time. Retention factor ($k'$), number of theoretical plates ($N$) and selectivity factor ($\alpha$) are the three parameters that control resolution. As one of the major elements in chromatographic separation, the stationary phase has a significant impact on all three parameters. A useful stationary phase should provide different selectivity with high efficiency and excellent reproducibility. Among the many types of stationary phases, silica-based phases are by far the most widely used for HPLC [1]. Some of the reasons for the popularity of silica substrate are: (1) their high efficiency resulting from good pore structure; (2) excellent mechanical strength; (3) good retention and a variety of selectivities. Stationary phases of all modes (e.g. reversed, normal, ion exchange, mixed-mode and size exclusion) can be prepared on silica substrates for use with compounds of various polarities, charge types and molecular weights [1–6].

However, the chemical stability of silica-based stationary phases at low pHs limit applications. At pHs lower than 2, siloxane bonds hydrolyze and the bonded organosilanes are released from the surface. The loss of the bonded phase and the generation of silanols leads to retention drift, increased peak width and tailing of organic cations [3,7,8]. Acid-stable HPLC stationary phases are particularly important for the separation of basic compounds, proteins and peptides, as acidic eluents are preferred for improved peak shape, as well as enhanced solubility and recovery. In addition, low pHs are the preferred conditions for LC–MS in the positive-ion mode; thus further increasing the need for improved acid stability.

A novel type of silica-based stationary phase with high acid stability has been developed in our lab [9–15]. A monolayer of a hyper-crosslinked (HC) aromatic network was synthesized on the silica substrate by means of a sequence of orthogonal polymer forming reactions. In this context we point out that most polymer forming reactions, e.g. free radical polymerization, take place between like molecules having similarly reactive functional groups. An orthogonal reaction takes place between two different kinds of functional groups that do not react with themselves. The only reaction possible is between unlike, i.e. orthogonal, reactants. The fully connected network polymer prevents the loss of bonded phase, thereby resulting in superior stability at low pH even compared to sterically protected phases, the phase having the best acid stability among currently available silica-based phases [10,11,15]. This greatly enhanced acid stability of HC phases not only ensures the

* Corresponding author. Tel.: +1 612 624 0253; fax: +1 612 624 7541.
*E-mail address:* petecarr@umn.edu (P.W. Carr).

0021-9673/$ – see front matter © 2011 Elsevier B.V. All rights reserved.
doi:10.1016/j.chroma.2011.07.096

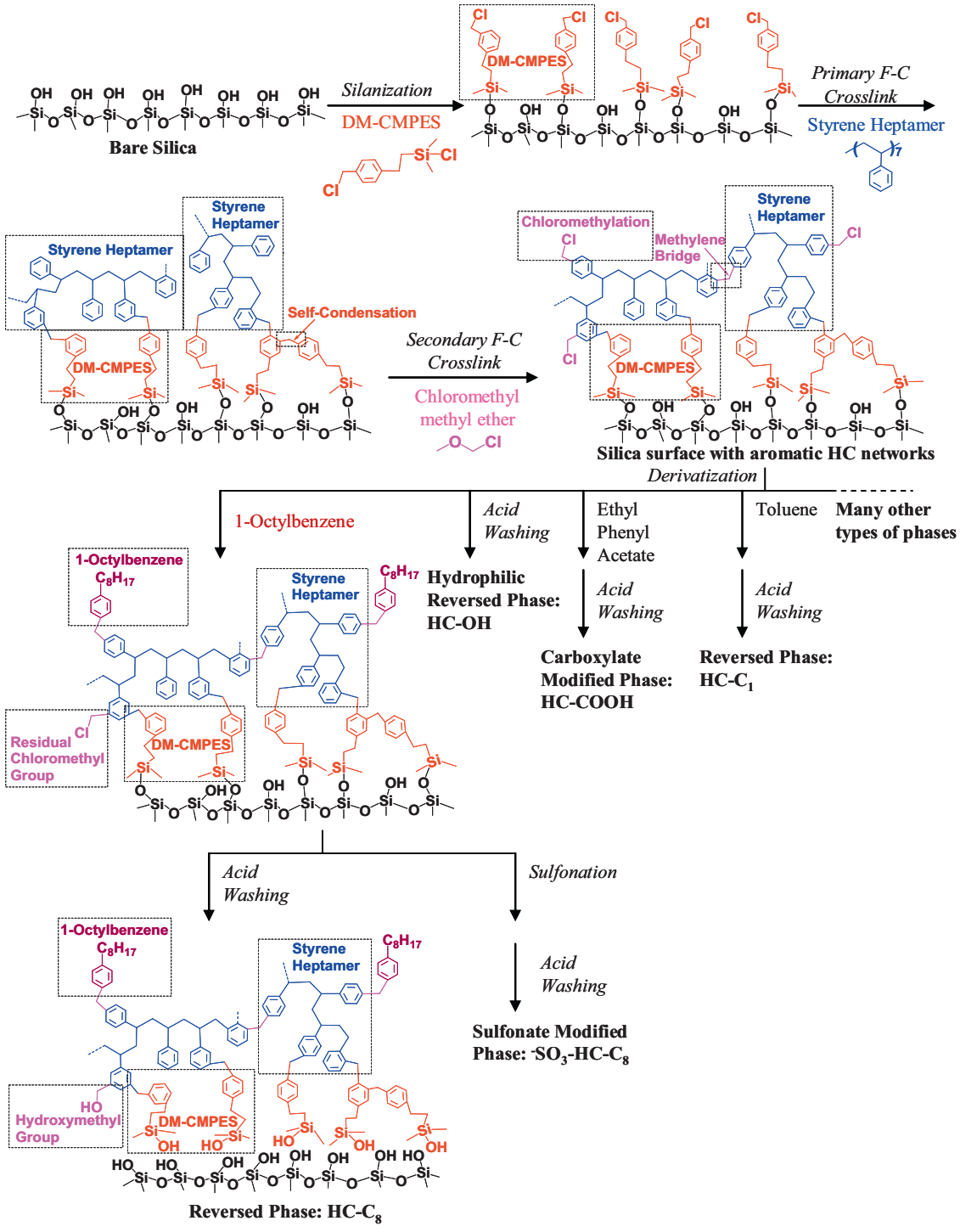


**Fig. 1.** General scheme to synthesize silica-based HC phases.

excellent reproducibility of retention and peak shape in separations at low pH, but it also makes ultra-fast high-temperature liquid chromatography (UFHTLC) possible. In UFHTLC, elevated column temperatures (>100 °C) are used to achieve dramatically reduced analysis times (e.g. <1 min) and much higher efficiencies at high velocity [16,17]. UFHTLC has been successfully used in the second dimension of 2D-LC, where extremely short run time is a prerequisite [18]. Additionally, high peak capacity can be generated in a short time by elevating the column temperature, which is essential for the separation of complicated samples such as protein tryptic digests [19].

More importantly, the use of orthogonal polymer forming reactions maintains the open pore structure of the silica substrate by confining the polymerization and crosslinking to silica's surface. Thus the high stability in acid is not achieved at the price of lower efficiency as is the case with polymer deposition and subsequent crosslinking [20–23]. No pore blockage was found and the HC phases provided plate counts comparable to conventional silica-based $C_{18}$ phases [10,15]. Additionally (see Fig. 1), the rich chemistry of the aromatic rings makes the hyper-crosslinked aromatic network an ideal platform for further functionalization to prepare different stationary phases with a wide variety of

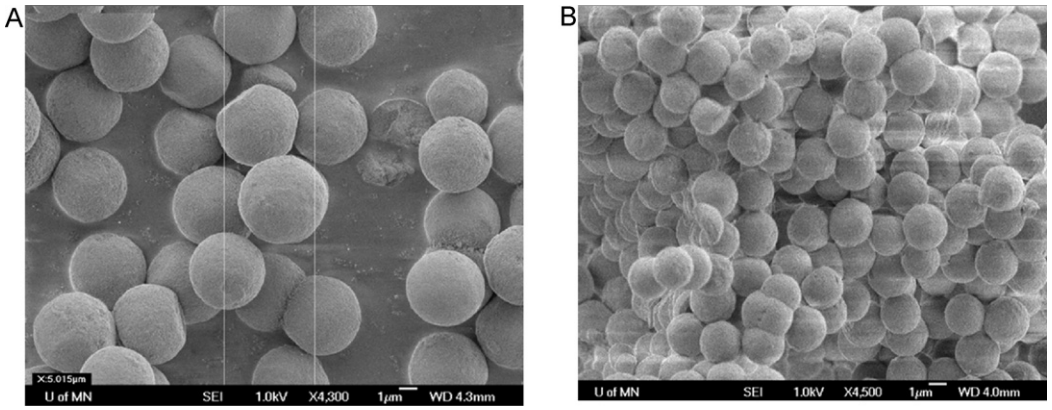


**Fig. 2.** SEM images of HC–$C_{8,\ Z\text{–}Al}$ particles before and after the removal of silica substrate. (A) HC–$C_{8,\ Z\text{–}Al}$ coated Zorbax silica particles before the HF digestion. (B) HC–$C_{8,\ Z\text{–}Al}$ coated Zorbax silica particles after the HF digestion to remove silica substrate.
Adapted from Ref. [11].

selectivity. HC reversed phases with various degrees of hydrophobicity and mixed-mode HC phases with added strong and weak cation exchange sites have been developed, characterized and applied [9–15].

## 2. Basic concept of hyper-crosslinked phases

### 2.1. Synthesizing a surface confined polymer network without blocking pores

For chromatographic stationary phases made on porous substrates, it is very important to make sure that the synthetic process does not result in significant pore blockage, especially when polymers and polymerization are involved in the surface modification [22,23]. It is well known that pore blockage can lead to poor mass transfer in the stationary zone, and thus low chromatographic efficiency [20,23].

Usually, the polymer deposition or growth cannot be easily controlled and pore blockage may occur on polymer-coated stationary phases and polymeric phases prepared using multifunctional organosilanes [22,24,25]. Unlike these types of phases, hyper-crosslinked phases were synthesized using a set of orthogonal reactions. The specific chemistry used here is similar to the Friedel–Crafts (FC) chemistry used by Davankov to form hyper-crosslinked polystyrene beads [26]. The use of orthogonal reaction chemistry circumvents pore blockage by completely confining the polymerization and crosslinking to within a monolayer of the silica surface. As shown in Fig. 1, the first step in our synthesis is the formation of a conventional monolayer of silane by modifying the surface with dimethyl-(p-chloromethylphenylethyl) chlorosilane (DM-CMPES). Key to our whole approach is the next step of first crosslinking the surface groups with a *multivalent reagent* (e.g. styrene heptamer or triphenyl methane) and secondly with a multi-functional alkylating reagent (e.g. chloro-methyl-methylether (CMME) or tribromomethyl mesitylene (TBM)) [10,12]. After these reactions the HC phases were extensively washed with a strong acid at high temperature. For this purpose we use 50/50 isopropanol:water with 5% TFA at 150 °C. Our goal is to *completely* hydrolyze all residual labile bonds, including all siloxane bonds and residual chloro methyl groups so as to stabilize the phase composition. This post-synthesis washing step further improves the acid stability.

A monolayer of extensively hyper-crosslinked polymer is indeed formed on the surface without any polymer generation in the pore or growth of polymer "perpendicular" to the surface. The absence of pore blockage has been confirmed by inverse size exclusion chromatography studies of the pore size distribution (see Table 1) [12]. This surface confined process yields a phase with superb mass transfer characteristics and excellent plate counts ($N$ > 100,000/m for 5 μm particles) [12].

While this chemistry is a good deal more complex than just the single silanization reaction needed to make a conventional bonded phase it has been done repeatedly by over a half dozen workers for nearly 10 years. The reactions are well known and easily controlled. The carbon loading has proven to be reasonably reproducible.

### 2.2. Increased acid and thermal stability of silica-based stationary phases

At low pHs (e.g. pH < 2), the silica substrate *per se* is very stable. However, the surface–ligand siloxane bonds on conventional monofunctional bonded stationary phases hydrolyze rather fast resulting in continual loss of bonded phase and drift in retention [3,7,8]. The use of higher temperatures accelerates phase loss. The acid stability of silica-based stationary phases can be enhanced either by sterically protecting the siloxane bonds with bulky side groups on the silane [8], or by increasing the number of siloxane bonds to the surface using "multi-dentate" and "multi-valent" silanes [8,27]. Hyper-crosslinked phases use a completely different concept for improving acid stability. An extensive aromatic *network* crosslinked by stable carbon-carbon bonds (see Fig. 1) is formed on the silica surface. The formation of the cross-linked network was verified by the SEM images of a hyper-crosslinked phase before and after the removal of all silica substrate. As indicated in Fig. 2, purely polymeric particles remained after the supporting silica skeletal framework was etched away. This hyper-crosslinked network is essential for the very high acid stability. The HC phases prepared in this way are remarkably more acid stable than sterically protected $C_{18}$ under exceedingly aggressive (50/50 acetonitrile/water with 5% TFA at 150 °C) aging conditions [10] (see Fig. 3). We point out that conventional bonded phases with short end-caps lose the short silane chains quite rapidly in acid. This is why many phases made for use in acid are not end-capped. For this reason we decided not to add an end-cap. In addition, the excellent thermal stability of the HC phases makes them good candidates for use in ultra-fast high temperature liquid chromatography and as the second dimension for fast 2D-LC [18]. For instance ultrafast gradient (<1 min) separations of proteins at 120 °C were enabled by this thermal stability [28].

**Table 1**
Calculated pore accessibility data for SB $C_{18}$ and the HC–$C_{8,\ Z-Al}$ stationary phases.

| Stationary phase | Percent carbon (±0.10%) | $V_{PORE}$ by ISEC | $V_{PHASE}$ by %C[a] (mL/column) | $V_{PHASE}$ by ISEC (mL/column) |
|---|---|---|---|---|
| Bare silica | 0.0 | 0.239 | 0.000 | 0.000 |
| SB $C_{18}$ | 10.1 | 0.176 | 0.107 | Not available[b] |
| HC–$C_{8,\ Z-Al}$ | 13.0 | 0.176 | 0.065 | 0.063 |

[a] A reasonable estimate for the density of the phases was used in the calculation (1.3 g/mL for the HC–$C_{8,\ Z-Al}$, 0.80 g/mL for SB $C_{18}$).
[b] The pore volume of the bare silica used for this stationary phase was not provided by the manufacturer (adapted from Ref. [13]).

### 2.3. A new platform for stationary phases of different selectivity

In addition to providing high acid stability and good mass transfer, the surface confined aromatic polymer network acts as a very useful platform for preparing a variety of stationary phases. A family of derivatized hyper-crosslinked phases with different functional groups (e.g. $C_8$, $C_1$, OH, $SO_3^-$, and COOH, see Fig. 1) have been synthesized and characterized [9,10,12,14,15]; they are discussed in the following sections. Characterization by the hydrophobic subtraction method (HSM) developed by Snyder and his collaborators [29] shows that the various HC phases have very different selectivity from commercial phases (Section 3.6.3). The diversity of the selectivity of the HC phases and their high acid stability enable various applications including the separation of pharmaceuticals [10,14], highly hydrophilic amines (e.g. catecholamines) [14,30], proteins and peptides [15,28], ultra fast separations at high temperatures [28], and use as both dimensions of 2D-LC.

## 3. Types of hyper-crosslinked phases

### 3.1. HC–$C_8$ phase using $AlCl_3$ as catalyst and Zorbax silica as substrate (HC–$C_{8,\ Z-Al}$)

Our first generation of acid-stable silica-based hyper-crosslinked phases was made using $AlCl_3$ as the catalyst in a sequence of orthogonal Friedel–Crafts reactions [12,13]. $AlCl_3$ is one of the strongest Friedel–Crafts catalysts and should result in the highest degree of crosslinking. As shown in Fig. 1, in the last functionalization step, 1-octylbenzene was reacted with residual benzyl chloride groups on the hyper-crosslinked aromatic network. This HC phase was prepared on Zorbax silica and is denoted as HC–$C_{8,\ Z-Al}$. HC–$C_{8,\ Z-Al}$ is rather more stable than sterically protected $C_{18}$ under extremely (5% trifluoroacetic acid, 150 °C) acidic conditions (see Fig. 3) [10,12]. Very significantly, the mass transfer kinetics of neutral compounds are comparable to those of monomeric silanized stationary phases, as demonstrated by the high plate counts and the small C term of the van Deemter equation for neutral compounds [12]. This indicates that orthogonal crosslinking does not plug pores. Good pore accessibility was further confirmed by the inverse size exclusion chromatographic (ISEC) studies of the pore size distribution [12]. The change in pore volume after modification can be calculated from ISEC data ($V_{PHASE,\ ISEC}$) and the stationary phase volume can be estimated from the measured carbon content ($V_{PHASE,\ \%C}$). If significant pore blocking were to occur, the $V_{PHASE,\ ISEC}$ would be larger than $V_{PHASE,\ \%C}$. If there were little or no pore blockage and the stationary phase were uniformly coated on the silica substrate, the $V_{PHASE,\ ISEC}$ should be approximately equal to the $V_{PHASE,\ \%C}$ [22,31]. The results of the volume comparison are given in Table 1. The $V_{PHASE,\ ISEC}$ of HC–$C_{8,\ Z-Al}$ is approximately equal to its $V_{PHASE,\ \%C}$, which is good evidence that the polymer formation is well confined to the silica surface and the synthesis of stationary phase does not lead to pore blockage [12].

The major drawback of HC–$C_{8,\ Z-Al}$ is that the peak widths for basic drugs were broader and sometimes the efficiency was considerably lower than observed with conventional $C_{18}$ columns [10,12]. We believed that an increased "silanophilicity" of the underlying silica due to Al(III) contamination was the major source of the poor performance of basic drugs. ICP-MS analysis show the presence of a considerable amount of Al(III) in the HC–$C_{8,\ Z-Al}$ even after aggressive post-synthesis acid washing [10]. Trace metals, especially Al(III), can significantly increase the acidity of silanols and cause bad peak shape of basic solutes [32,33]. This poor performance was also evident in the separation of some proteins in acidic eluents [28].

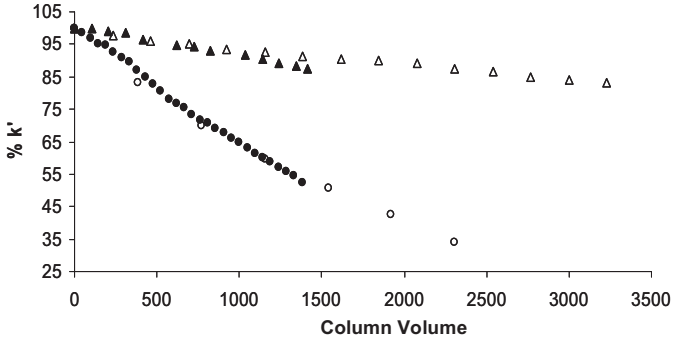


**Fig. 3.** Stability comparison of the HC–$C_{8,\ Hi-Sn}$ phase, the HC–$C_{8,\ Z-Al}$ phase, and the SB $C_{18}$ phase. The stability test conditions for SB $C_{18}$ and HC phases: 5% TFA in 50/50 ACN/water, $T$ = 150 °C. △: (3.3 cm × 0.21 cm) the HC–$C_{8,\ Hi-Sn}$ phase was aged at a flow rate of 0.5 mL/min with hexadecanophenone as probe; ▲: (5.0 cm × 0.46 cm) the HC–$C_{8,\ Z-Al}$ phase was aged at a flow rate of 2.0 mL/min with dodecanophenone as probe; ○: (3.3 cm × 0.21 cm) the SB $C_{18}$ phase was aged at a flow rate of 0.5 mL/min with hexadecanophenone as probe; ●: (5.0 cm × 0.46 cm) the SB $C_{18}$ phase was aged at a flow rate of 2.0 mL/min with dodecanophenone as probe.
Adapted from Ref. [10].

### 3.2. HC–$C_8$ phase using $SnCl_4$ as catalyst and HiChrom silica as substrate (HC–$C_{8,\ Hi-Sn}$)

As mentioned in the preceding section, the performance of basic analytes on HC–$C_{8,\ Z-Al}$ phases was poor compared to that of conventional silica-based $C_{18}$ phases. This problem was essentially solved by replacing $AlCl_3$ with $SnCl_4$ (a less effective but still strong Friedel–Crafts catalyst [26]) and by use of a better grade of Type-B silica from HiChrom. Using ACN/water with 0.1% TFA, the plate count for amitryptyline increased from 2100 to 3700 with Zorbax silica as the substrate but using $SnCl_4$ instead of $AlCl_3$. Furthermore, upon changing from Zorbax to HiChrom silica with $SnCl_4$ as the catalyst on both substrates increased the plate count from 3700 to 4600. Using $SnCl_4$ and HiChrom silica, the plate counts for bases are virtually as good as those for neutral solutes (4500–5000).

The efficiency of a series of different basic analytes on the new generation of HC–$C_8$ phase synthesized with $SnCl_4$ catalyst and HiChrom silica (HC–$C_{8,\ Hi-Zn}$) was further compared with three commercial stationary phases, SB $C_{18}$, ACE $C_{18}$ and Inertsil ODS3. The latter two phases are noted for their very low silanol activity. The weak ion-pairing reagent [34], formic acid, was used as the buffer to better differentiate the performance of different phases that would be obscured by stronger ion pairing reagents such as trifluoroacetic acid (TFA). Fig. 4 shows that the HC–$C_{8,\ Hi-Sn}$ phase had

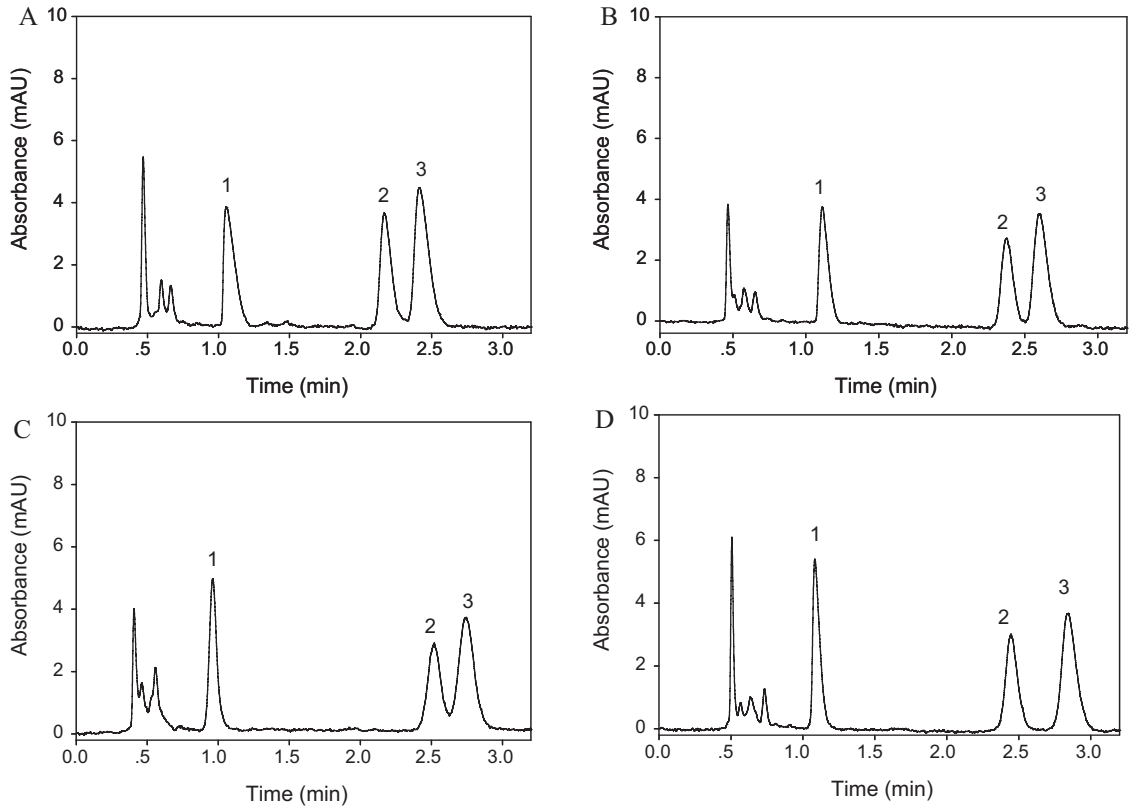


**Fig. 4.** Silanophilicity comparison of the HC–$C_{8,\,Hi-Sn}$ phase, the SB $C_{18}$, the ACE $C_{18}$, and the Inertsil ODS 3 phases. Separation of alprenolol, nortriptyline, and amitriptyline were done on (A) SB $C_{18}$ ($N_{amitriptyline}$ = 2750), (B) ACE $C_{18}$ ($N_{amitriptyline}$ = 3400), (C) Inertsil ODS3 ($N_{amitriptyline}$ = 3000), and (D) HC–$C_{8,\,Hi-Sn}$ ($N_{amitriptyline}$ = 3800), %ACN was varied to make $k'$ similar on all phases. For the HC–$C_{8,\,Hi-Sn}$ phase and ACE $C_{18}$ $\phi_{ACN}$ = 34%; for SB C18 $\phi_{ACN}$ = 38%; for Inertsil ODS $\phi_{ACN}$ = 16.3%. All columns have the same dimension of 5 cm × 0.46 cm and similar plate count for neutral compounds. $T$ = 40 °C, $F$ = 1 mL/min, $\lambda$ = 254 nm. 0.1–0.2 nmol of samples were injected. (1) alprenolol, (2) nortriptyline, and (3) amitriptyline.

the highest plate counts for all bases despite not being endcapped [10].

The acid stability of the HC–$C_{8,\,Hi-Sn}$ phase was tested and compared with the acid stability of HC–$C_{8,\,Z-Al}$ and the sterically protected SB $C_{18}$ phase. The same exceedingly aggressive acid aging conditions (5% TFA and 150 °C) was used for this comparison. The results are shown in Fig. 3. The HC–$C_{8,\,Hi-Sn}$ phase shows comparable acid stability to the HC–$C_{8,\,Z-Al}$ phase, and both are much more stable than the sterically protected $C_{18}$ phase [10].

### 3.3. A hydrophobically assisted strong cation exchange phase (–$SO_3$–HC–$C_8$)

A novel type of silica-based sulfonated mixed-mode phase –$SO_3$–HC–$C_8$ was developed by lightly sulfonating the aromatic hyper-crosslinked network of HC–$C_{8,\,Hi-Sn}$ [9,30]. Controlling the sulfonation temperature allows control of the degree of sulfonation: approximately 0.4 and 0.1 μmol/$m^2$ of sulfonyl groups were introduced at −41 °C and −61 °C, respectively during 30 min of reaction. These low levels of sulfonation did not significantly decrease the phase hydrophobicity but they did provide additional cation exchange activity which differentiates the sulfonated phases from all other RPLC phases [9]. Moreover, the selectivity of this phase for cations is significantly enhanced by its high hydrophobicity through a "hydrophobically assisted" ion exchange retention process [30,35]. This aids the separation of highly hydrophilic bases which are hard to separate by conventional RPLC phases due to their very low retention. One of the important uses of the –$SO_3$–HC–$C_8$ phase is the separation of catecholamines [30]. Nine catecholamine compounds were separated on three different phases: a conventional reversed phase (SB $C_{18}$), a commercial mixed-mode phase (Primesep 200) and the –$SO_3$–HC–$C_8$ phase. Fig. 5 shows that most catecholamines were poorly retained and not baseline separated on SB $C_{18}$ even with 10 mM hexanesulfonate, a strong ion paring agent, and only 10% acetonitrile in the eluent. The cation exchange sites on both Primesep 200 and –$SO_3$–HC–$C_8$ phase result in the substantially increased retention. Due to its higher hydrophobicity, the –$SO_3$–HC–$C_8$ phase provides a separation superior to that of Primesep 200, which was designed especially for catecholamines. Some of the most interesting features of –$SO_3$–HC–$C_8$ are: (1) both neutral compounds and charged bases can be simultaneously separated; (2) gradients in either organic modifier or salt concentration can be used to effect the separation of a wide range of solutes [30]; and (3) the unusual fact that organic bases are always more retained than are related uncharged solutes.

### 3.4. A hydrophobically assisted weak cation exchange phase (HC–COOH)

A mixed-mode reversed-phase/weak cation exchange (RP/WCX) phase was developed by introducing a small amount of a carboxylate functionality into the hydrophobic hyper-crosslinked (HC) platform made using $SnCl_4$ as catalyst and HiChrom silica as substrate [14]. After an hour of reaction with ethyl phenyl acetate at 80 °C, 0.5 ± 0.1 μmol/$m^2$ of phenyl acetate groups were attached to the aromatic network. The esters were hydrolyzed into the corresponding phenyl acetic acids during the gradient hot acid washing step.

Compared to the previously developed –$SO_3$–HC–$C_8$ phase the added carboxylic groups impart *weak cation* exchange selectivity

**Table 2**
Effect of column type on efficiency, sample loading capacity, and retention of basic drugs.[a]

| Solutes[a] | HC–COOH | | | | ACE $C_{18}$ | | | | $N_0$ (HC–COOH)/$N_0$ (ACE $C_{18}$) | $w_{1/2}$ (HC–COOH)/$w_{1/2}$ (ACE $C_{18}$) |
|---|---|---|---|---|---|---|---|---|---|---|
| | $k'$ | $N_0$[b] | $w_{1/2}$ (nmol)[b] | $r^2$[b] | $k'$ | $N_0$[b] | $w_{1/2}$ (nmol)[b] | $r^2$[b] | | |
| Methamphetamine | 5.12 | 3680 | 77.4 | 0.885 | 3.90 | 2950 | 3.4 | 0.997 | 1.25 | 22.7 |
| MDMA | 5.58 | 3450 | 26.9 | 0.987 | 4.19 | 2980 | 3.0 | 1.000 | 1.16 | 9.1 |
| MDA | 4.21 | 3430 | 89.7 | 0.968 | 3.38 | 2960 | 3.0 | 0.999 | 1.16 | 30.2 |
| Methcathinone | 3.79 | 3490 | 190.0 | 0.978 | 2.21 | 2730 | 9.9 | 0.992 | 1.28 | 19.2 |
| MDEA | 6.56 | 3310 | 34.9 | 0.998 | 6.56 | 3110 | 5.0 | 1.000 | 1.06 | 7.0 |

[a] Structures of the basic solutes are shown in Ref. [16]. Chromatographic conditions: (a) ACE $C_{18}$ column: 5 mM ammonium acetate in 10/90 (v/v) ACN/water, pH 6.08; (b) HC–COOH column: 5 mM ammonium acetate in 40/60 (v/v) ACN/water, pH 5.96; other chromatographic conditions: 5.0 cm × 0.46 cm column, $T$ = 40 °C, $F$ = 1.0 mL/min; wavelength = 210 nm.

[b] The limiting plate count ($N_0$) and sample loading capacity ($w_{0.5}$) calculated from the following equation using the corresponding data given in Fig. 12 from Ref. [14]:

$$\frac{N}{N_{0.5}} = \frac{1 + 1.489\omega'}{1 + 1.489\omega' + 2.489\omega'^2}.$$

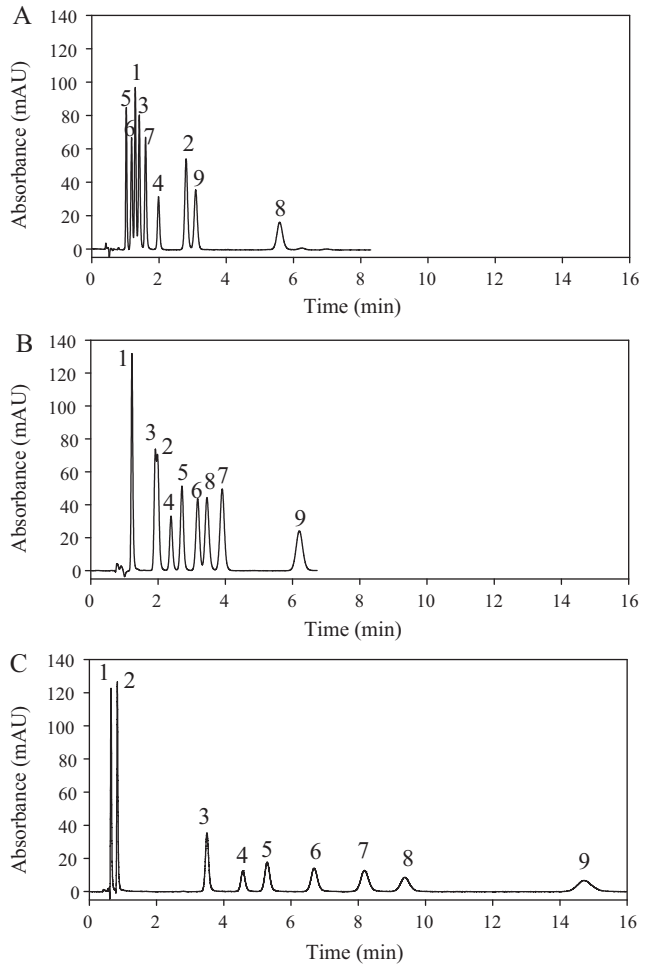


**Fig. 5.** The chromatograms of the separation of catecholamines on different phases. (A) SB $C_{18}$. Chromatographic conditions: 10/90 ACN/$H_2O$ containing 0.1% (v/v) TFA, 0.2 mM EDTA and 10 mM sodium hexanesulfonate, $T$ = 40 °C. (B) Primesep 200. Chromatographic conditions: 10/90 ACN/$H_2O$ containing 0.02% (v/v) TFA, $T$ = 40 °C. (C) –$SO_3$–HC–$C_8$. Chromatographic conditions: 24/76 ACN/$H_2O$ containing 0.02% (v/v) TFA and 0.2 mM EDTA, $T$ = 65 °C. Other chromatographic conditions: 5.0 cm × 0.46 cm column, $F$ = 1.0 mL/min. Solutes: (1) 3,4-dihydroxyphenylacetic acid; (2) homovanillic acid; (3) 3.4-dihydroxy-L-phenylalanine; (4) tyrosine; (5) norepinephrine; (6) epinephrine; (7) dopamine; (8) phenylalanine; (9) 3-methoxytyramine.
Adapted from Ref. [9].

to the base hydrophobic HC platform and make it possible to analyze the basic solutes on the HC–COOH phase using formic acid and acetic acid buffers as eluents [14]. This avoids the mass spectrometric ionization suppression problems concomitant to the use of non-volatile additives such as triethylamine or inorganic salts needed to elute bases from the strong cation exchange phase. The carboxylate phase also offers the flexibility that gradients in organic modifier, pH or ionic competitors can be used to affect the separation of a wide range of solutes. For example, the separation of hydrophilic neurotransmitters and drugs of abuse were achieved with simple ammonium acetate buffers without the need for ion pairing agents [14]. In contradistinction, the weak cation exchange phase had sufficient retention and excellent efficiency. Additionally, the HC–COOH phase showed radically different selectivity when compared to a conventional $C_{18}$ phase and the strong cation exchange phase –$SO_3$–HC–$C_8$ [14]. It is noteworthy that the HC–COOH phase also provided an order of magnitude increase in loading capacity (Table 2) when compared to conventional alkyl-silica phases [14].

### 3.5. The third generation: the HC–T phase

One of the most challenging applications for the HC phases is the separation of proteins and peptides. As discussed in Section 3.2 upon replacing $AlCl_3$ with $SnCl_4$ and using a better grade of Type-B silica, the second generation HC phase achieved more than twice the plate count of the first generation phase for basic drugs. However, tin(IV) contamination still takes place during the synthesis of the silica [36,37]. This became evident when a mixture of peptide standards was separated on HC–$C_{8,\ Hi-Sn}$. Considerably wider peak widths (20–30%) and lower plate counts were still observed on HC–$C_{8,\ Hi-Sn}$ compared to conventional bonded $C_{18}$ columns [36].

In order to further reduce the amount of tin contamination, kinetic studies were performed on each of the three Friedel–Crafts processes. The chief result of this study was an optimized set of reaction conditions. In the primary crosslinking step, triphenyl methane was used in place of heptyl styrene. In the secondary crosslinking process 2,4,6-tris(bromomethyl)-mesitylene was used instead of chloro-methyl-methylether. Toluene replaced octylbenzene in the last step [15]. Use of these new crosslinking and derivatization reagents and much higher reagent concentrations allowed significant reductions in reaction times leading to even lower silanolphilicity [15].

The "HC–T" phase represents the third generation of the HC phases. The efficiency of the new phase was tested using a series of basic analytes (i.e. amitriptyline, nortriptyline and alprenolol); the HC–T phase showed a 30% increase in plate count as compared to the HC–$C_{8,\ Z-Sn}$ phase. The silanolphilicity of the new phase was def-

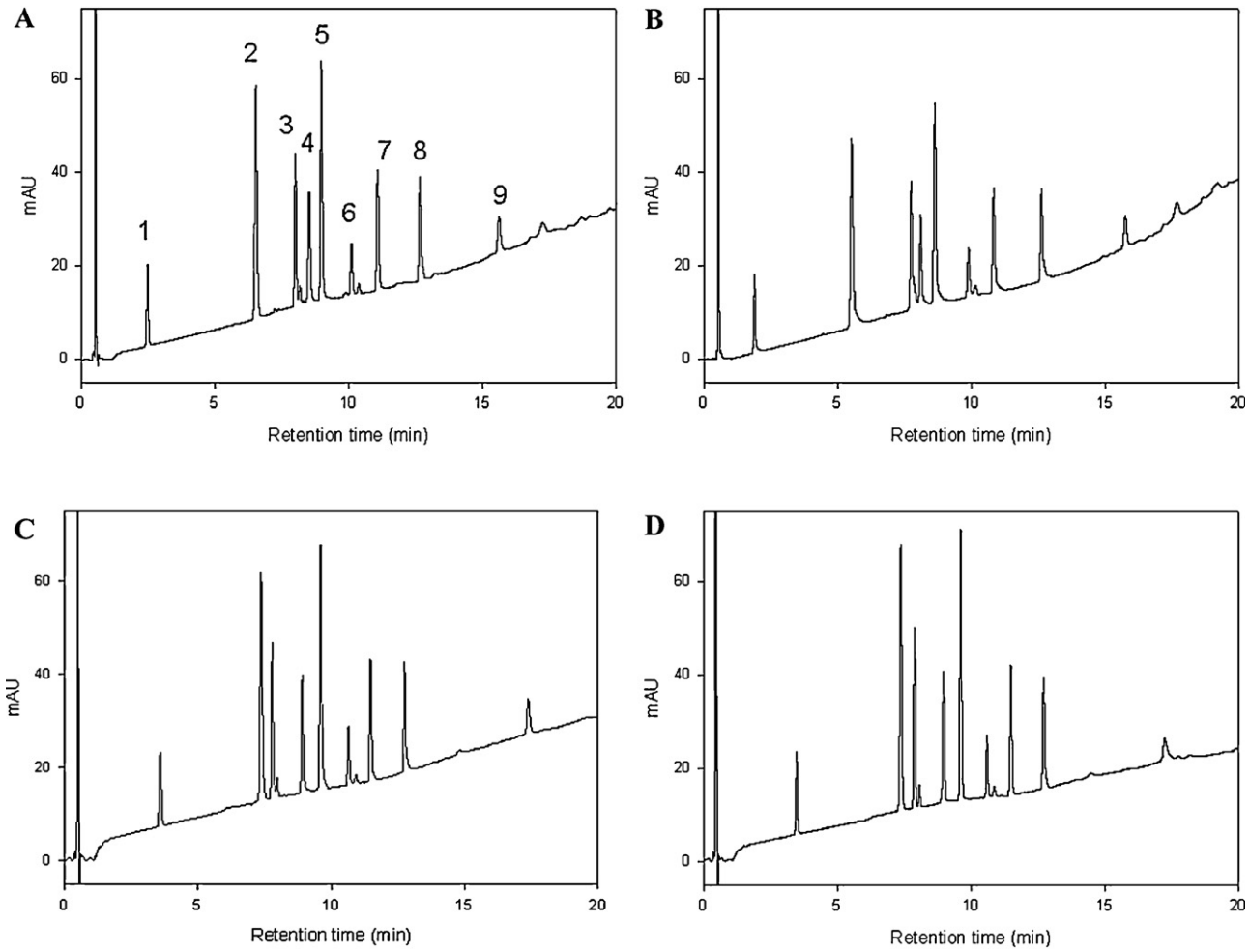


**Fig. 6.** Comparison of separation efficiencies of the HC–T, the HC–$C_{8,\,Z\text{–}Sn}$, the SB $C_{18}$ and the ACE $C_{18}$ phases with peptide standards. Chromatographic conditions: All columns (5.0 cm × 0.46 cm) are packed with 5 μm particles. Mobile phases: solvent A: 0.1% formic acid in 5/95 (v/v) ACN/water, solvent B: 0.1% formic acid in 55/45 (v/v) ACN/water. Gradient profile: 0.00–15.00 min 10–80% B, 15.00–15.01 min 80–10% B, 15.01–22.00 min 10% B. $F$ = 1.4 mL/min, Temp = 40 °C, λ = 214 nm. Nine peptides mixture (0.01–0.08 mg/mL) 5 μL injection. Solutes: (1) Gly-Phe; (2) Phen-Phe; (3) LHRH Human; (4) Angiotensin II; (5) [$Val^5$]-Angiotensin; (6) Substance P; (7) Renin Substrate; (8) Insulin Chain B; (9) Melittin; (A) HC–T; (B) HC–$C_{8,\,Z\text{–}Sn}$; (C) ACE $C_{18}$; (D) SB $C_{18}$.
Adapted from Ref. [15].

initely reduced by optimizing the synthesis conditions [15]. Fig. 6 compares peptide separations on the HC–T, HC–$C_{8,\,Z\text{–}Sn}$ and several commercial stationary phases. The HC–$C_{8,\,Z\text{–}Sn}$ phase gave the widest peaks. On the other hand, the separation efficiency of peptides on the HC–T phase was significantly improved and is now comparable to if not superior to the SB $C_{18}$ and ACE $C_{18}$ phases [15].

The HC–T phase has shown some distinctive selectivity relative to both conventional RP phases and other HC type phases. For example, the HC–T phase was used to analyze a petroleum sample [38]. The new phase showed unique normal phase selectivity for nitrogen group-types and polycyclic aromatic hydrocarbons (PAHs), attaining a separation under gradient conditions in less than 30 min (Fig. 7). Such novel selectivity, combined with high efficiency and chemical stability, would make the third generation HC–T phase a good candidate in the separations of bases or biological analytes in acidic media, especially at elevated temperatures.

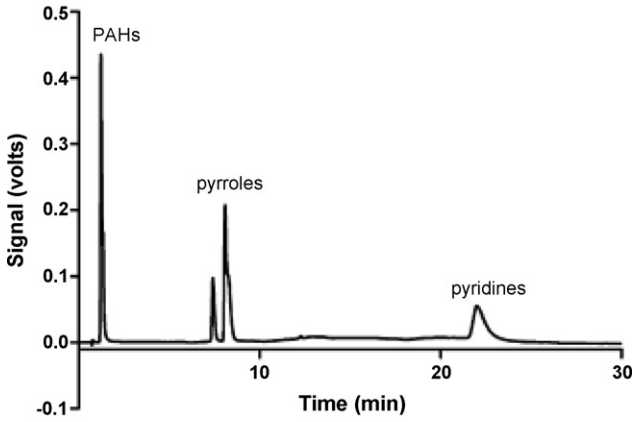


**Fig. 7.** Chromatogram of nitrogen/PAH mix under a step gradient on the HC–T column. Temperature was 35 °C, at a flow rate of 1 mL/min, detection wavelength of 254 nm. PAHs: benzene, pyrene, anthracene. Pyrroles: indole, carbazole, 1H-benzo[g]indole. Pyridines: quinoline, phenanthridine, acridine. Step gradient was 20 min long, with 12 min of equilibration time. Initial solvent condition was 5% DCM in hexane, increasing by 20% DCM every 4 min. Equilibration time was 12 min between each gradient separation [39].

### 3.6. The polar HC–OH phase

Recently, a more hydrophilic reversed phase (the HC–OH phase) was developed based upon the HC platform using $SnCl_4$ as the catalyst and HiChrom silica as the substrate. As shown in Fig. 8, the

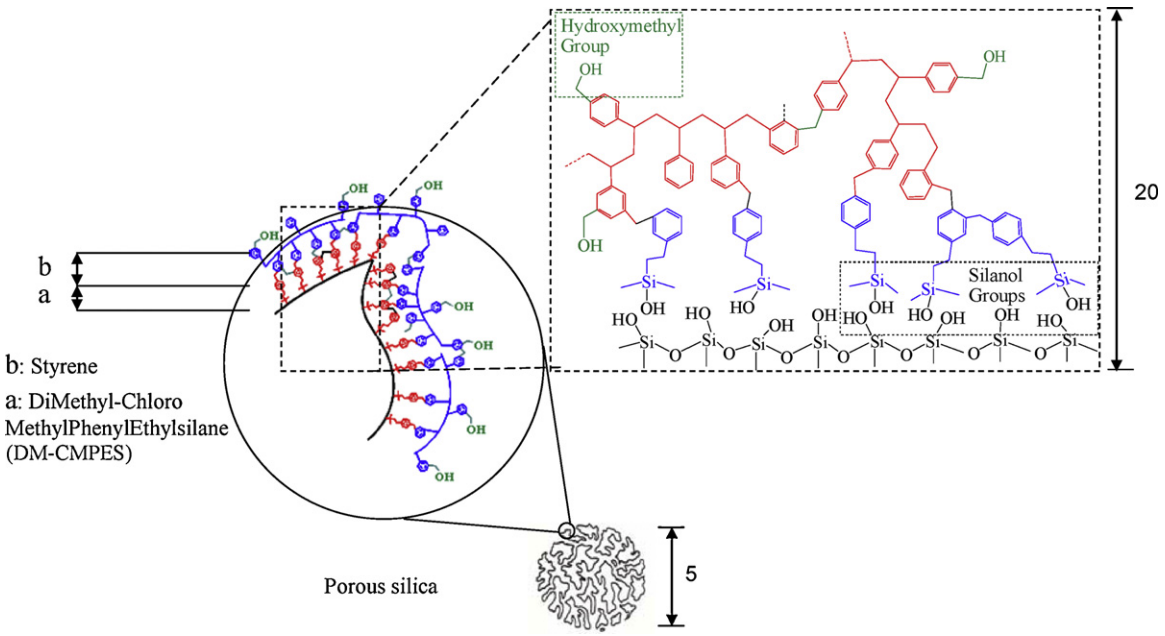


**Fig. 8.** Schematic illustration of chemical structure of the HC–OH phase.

new phase has a benzylic hydroxyl functionality embedded into the HC platform. The hyper-crosslinked polymer network provides hydrolytic stability while the $3.3 \pm 0.1$ μmol/m$^2$ of polar groups make the HC–OH more compatible with water rich mobile phases and introduce additional mode of polar selectivity. The resulting material exhibits several distinctive chromatographic properties including:

(1) Thermal and hydrolytic stability provided by the hyper-crosslinked polymer network;
(2) Improved performance for basic compounds compared to conventional $C_{18}$ phases;
(3) A novel selectivity offered by an aromatic network combined with a high density of polar benzylic hydroxyl groups ($3.3 \pm 0.1$ μmol/m$^2$).

These properties make the new polar phase a very good candidate for use as the first dimension of 2D-RP separations. Fig. 9 shows a sample RP × RP chromatogram of a maize seed extract where the HC–OH phase and a ZirChrom-CARB phase were used as the first and second dimensions, respectively. More than 100 metabolites peaks were observed in a single maize seed extract. This demonstrates the tremendous power of the 2D-HPLC technique in dealing with complex biological samples. The advantages of selecting the HC–OH phase as the first dimension column of 2DLC are:

(1) Long term retention stability and fewer artifacts due to column bleed are seen in the second dimension chromatogram (comparative data not shown here);
(2) The novel selectivity allows a higher degree of orthogonality of the separation selectivities to be achieved when a carbon clad phase is used in the second dimension (Fig. 9);
(3) The mobile phase used on the hydrophilic first dimension column is much weaker than what must be used on a $C_{18}$ phase, which minimizes the excessive peak broadening on the second dimension caused by the "strong solvent injection effect" [18].

The preparation and characterization of this polar-embedded stationary phase is discussed in the following sections.

### 3.6.1. Preparation and characterization of the HC–OH phase

The synthesis of the HC–OH phase is shown in Fig. 1 and the product at each stage was characterized by elemental analysis (Table 3). The first three steps in our preparation are the same as the HC–$C_{8,\,Hi-Sn}$ phase: a conventional monolayer of silane is first formed as usual by covalently bonding $3.0 \pm 0.1$ μmol/m$^2$ of dimethyl-(p-chloromethylphenylethyl) chlorosilane (DM-CMPES) to the silica surface. Then by reacting the surface benzyl chloride groups with first a multi-valent aromatic reagent ($0.3 \pm 0.1$ μmol/m$^2$ styrene heptamer) and secondly with a bi-functional alkylation reagent ($3.6 \pm 0.1$ μmol/m$^2$ chloromethyl-methylether (CMME)), a crosslinked network polymer was

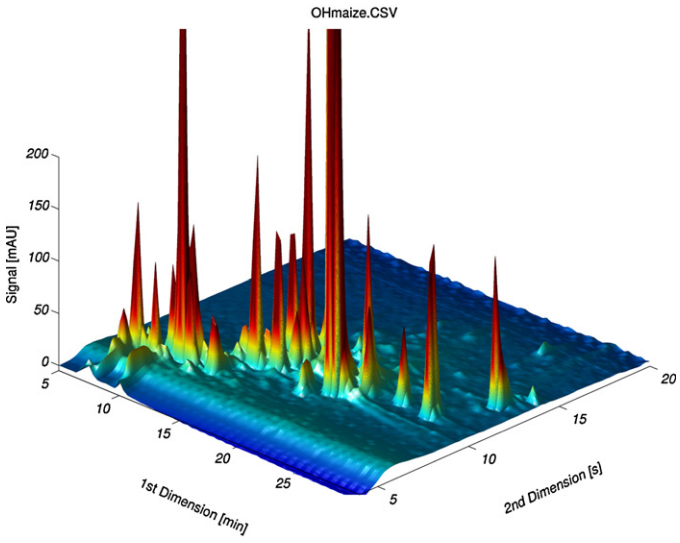


**Fig. 9.** 2D-HPLC separation of unpurified extract of corn seedling tissue. The entire analysis is completed in 40 minutes, and over 100 chromatographic peaks are observed using UV detection. First dimension: 50 mm × 2.1 mm. i.d., HC–OH, 0.10 mL/min; gradient: 0%B–50%B from 0.0 to 24.0 min; solvent A: 1.5 mM phosphoric acid; solvent B: acetonitrile; 40 °C; detection at 220 nm. Second dimension: 50 mm × 2.1 mm. i.d., ZirChrom CARB, 3.0 mL/min; gradient: 0%B–100%B from 0.0 to 0.30 min; solvent A: 10 mM phosphoric acid; solvent B: acetonitrile; 110 °C; detection at 220 nm.

**Table 3**
Summary of elemental analysis at each step in the synthesis of the HC–OH and the HC–$C_{8,\ Hi-Sn}$ phases.

| Phase designation | Elemental analysis (w/w) | | Surface coverage (μmol/m$^2$) | | |
|---|---|---|---|---|---|
| | %C[a] | %Cl[b] | Chloromethyl[c] | Octyl[d] | Benzylic hydroxyl[e] |
| HC-platform[f] | 11.21 | 1.92 | 2.5 | N/A | N/A |
| HC–OH | 11.76 | <0.25 | ND[g] | N/A | 2.5 |
| HC-platform[f] | 11.00 | 2.09 | 2.8 | N/A | N/A |
| HC–$C_{8,\ Hi-Sn}$ | 14.43 | 0.71 | 1.0 | 1.0 | N/A |
| HC–$C_{8,\ Hi-Sn}$ after acid washing | 14.84 | 0.26 | 0.4 | 1.1 | N/A |

[a] Detection limit is 0.10% (w/w).
[b] Detection limit is 0.25% (w/w).
[c] Surface coverage of chloromethyl groups based on chlorine analysis.
[d] Surface coverage of octyl groups based on carbon analysis.
[e] Surface coverage of hydroxylmethyl groups based on chlorine analysis.
[f] HC platform prepared on HiChrom silica using $SnCl_4$ as the Friedel–Crafts catalyst in the synthesis from Ref. [10].
[g] Below detection limit.

formed on the silica surface. The detailed reaction conditions of the silanization and Friedel–Crafts crosslinking steps can be found in previous publications [10,14]. Upon completion of the secondary crosslinking, there were approximately 2.5 ± 0.1 μmol/m$^2$ of residual chlorobenzyl groups on the silica surface. Exhaustively treating the HC-platform with a "gradient" washing procedure at pH 0.5 and 150 °C fully hydrolyzed the residual benzylchloride groups into benzylic hydroxyl groups to form the HC–OH phase. Table 3 shows that nearly all the chloride groups were removed after this aggressive acid treatment, which suggests that the benzylchloride groups were almost completely converted into benzylic hydroxyls. Thus we estimate there are about 2.5 ± 0.1 μmol/m$^2$ of benzylic hydroxyl groups. There were minimal losses in the carbon content of the HC–OH and HC–$C_{8,\ Hi-Sn}$ phases (Table 3) before and after the "gradient" washing procedure. This indicates that there was essentially no loss in the amount of bonded phase during the acid treatment which further confirms the existence of the hyper-crosslinked network on the particle surface.

Based on the negligible loss in carbon we believe that the decrease in retention of non polar solutes upon accelerated aging (Fig. 3) is not due to loss in bonded phase as is the case with conventional bonded phases but rather is due almost entirely to the very slow hydrolysis of residual Si–O–Si bonds. This generates additional SiOH groups on both the silica and the silane. This is supported by the strong silanol activity observed on all HC-based phases (Section 3.6.3.3).

### 3.6.2. Linear solvent strength characterization

The hydrophobicity of the HC–OH phase was first assessed by looking at the free energy of transfer per methylene unit. This is the ability of a phase to distinguish between two compounds based upon a single methylene unit addition, and was determined by injecting a series of homologs [39]. The slope, $B$, of a plot of $\log k'$ versus the number of $CH_2$ groups (Fig. 10) was used to calculate the free energy of transfer per methylene unit via the following equation:

$$\Delta G^{\circ}_{CH_2} = -2.3RTB \quad (1)$$

The slopes, intercepts and free energies of the transfer per methylene group for the HC–OH phases are summarized in Table 4 to compare this phase with several others. The hydrophobicity (represented by $\Delta G^{\circ}_{CH_2}$) follows the order: HC–OH < HC–COOH < –$SO_3$–HC–$C_8$ < HC–$C_{8,\ Hi-Sn}$ < SB $C_{18}$. Among the four HC phases, the reversed HC–$C_{8,\ Hi-Sn}$ phase showed the highest hydrophobicity presumably due to the presence of 1.0 ± 0.1 μmol/m$^2$ of hydrophobic octyl chains; this hydrophobicity decreases about 10% upon introduction of the polar sulfonyl groups based on comparison of $\Delta G^{\circ}_{CH_2}$ of –$SO_3$–HC–$C_8$ vs. HC–$C_{8,\ Hi-Sn}$. On the other hand, both the HC–COOH and HC–OH phases displayed significantly lower hydrophobicities than the other two phases. The lower hydrophobicity of the HC–COOH phases is mainly due to the absence of the hydrophobic octyl chain. The HC–OH phase hydrophobicity is further reduced by the presence of 2.5 ± 0.1 μmol/m$^2$ polar benzylic hydroxyl groups. As a result, the $\Delta G^{\circ}_{CH_2}$ of the HC–OH phase is only about 66% of that of HC–$C_{8,\ Hi-Sn}$ phase and 57% of that of a commercial $C_{18}$ phase. This is quite useful in LC × LC in that it lowers the amount of strong solvent needed to elute samples and enables better focusing on the second dimension column [18].

### 3.6.3. Selectivity characterization by the Hydrophobic Subtraction Model (HSM)

The retention behavior of a phase is determined by both the hydrophobic interactions between the bonded phase and the solute analyte as well as by the various hydrophilic interactions including hydrogen bonding, dipole interactions and ion-exchange interactions with basic/polar functional groups of the analyte. To understand these fundamental chromatographic characteristics of the HC–OH phase, its selectivity was characterized using the Hydrophobic Subtraction Model [29,40–47]:

$$\log\left(\frac{k}{k_{EB}}\right) \equiv \log\alpha = \underset{(i)}{\eta' H} - \underset{(ii)}{\sigma' S^*} + \underset{(iii)}{\beta' A} + \underset{(iv)}{\alpha' B} + \underset{(v)}{\kappa' C} \quad (2)$$

In Eq. (2) the relative retention of a solute $k/k_{EB}$ on a reversed phase column is separated into contributions from various types of intermolecular interactions [29,40–47]. These are: hydrophobic interactions (i); steric resistance of the stationary phase to insertion

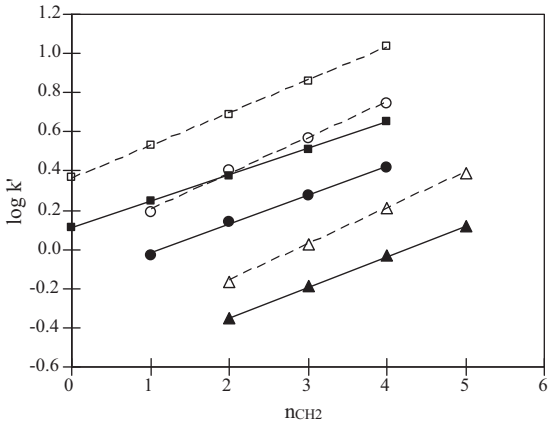


**Fig. 10.** Plots of $\log k'$ vs. number of methylene groups on HC–OH phase and HC–$C_{8,\ Hi-Sn}$ phase. Chromatographic conditions: 50/50 ACN/water, 5.0 cm × 0.46 cm column, $T$ = 35 °C, $F$ = 1.0 mL/min. HC–OH: (▲) alkylacetate homolog; (●) alkylphenone homolog; (■) alkylbenzene homolog. HC–$C_{8,\ Hi-Sn}$: (△) alkylacetate homolog; (○) alkylphenone homolog; (□) alkylbenzene homolog.

**Table 4**
The slopes and intercepts of $\log k'$ vs. $n_{CH_2}$, and $\Delta G_{CH_2}{}^{\circ}$ obtained on various HC phases for the separation of alkylphenone homologs.

| Stationary phases | Slope | Intercept | $r^2$ | SE | $\Delta G_{CH_2}{}^{\circ}$ (cal mol$^{-1}$)[d] |
|---|---|---|---|---|---|
| SB $C_{18}$[a] | 0.226 ± 0.0006 | −0.073 ± 0.003 | 1.0000 | 0.002 | −324 ± 0.9 |
| HC–$C_{8,\ Hi-Sn}$[a] | 0.195 ± 0.0006 | 0.100 ± 0.003 | 1.0000 | 0.001 | −280 ± 09 |
| –$SO_3$–HC–$C_8$[b] | 0.183 ± 0.0002 | −0.033 ± 0.001 | 1.0000 | 0.001 | −262 ± 0.3 |
| HC–COOH[a] | 0.147 ± 0.0004 | −0.003 ± 0.002 | 1.0000 | 0.001 | −210 ± 06 |
| HC–OH[c] | 0.136 ± 0.0009 | −0.003 ± 0.005 | 0.9997 | 0.004 | −185 ± 1.2 |

[a] Data is adapted from Ref. [14]. Chromatographic condition: 50/50 ACN/water with 0.1% formic acid, 5.0 cm × 0.46 cm column, $T$ = 40 °C, $F$ = 1.0 mL/min.
[b] Data is adapted from Ref. [14]. Chromatographic condition: 50/50 ACN/water with 0.1% formic acid and 10 mM TEA. HCl, 5.0 cm × 0.46 cm column, $T$ = 40 °C, $F$ = 1.0 mL/min.
[c] Chromatographic condition is the same as in Fig. 10. The slope, intercept standard error and the squared correlation coefficient of the linear regression of $\log k'$ vs. nCH2 are calculated based on the data in Fig. 10.
[d] The free energy of transfer per methylene group calculated from Eq. (1) using the corresponding slope.

of the bulky molecules (ii); hydrogen bonding (HB) donor solutes with HB acceptor groups on the column or HB acceptor solute with HB donor groups on the column (iii)–(iv); and Coulombic interactions (v). A set of 16 judiciously selected but chemically simple probe solutes were used to characterize the chromatographic system by these interactions. $H$, $S^*$, $A$, $B$ and $C$ are the column selectivity parameters and $\eta'$, $\sigma'$, $\beta'$, $\alpha'$ and $\kappa'$ are the corresponding solute properties.

The new HC–OH phase was studied and compared with the other HC-based phases and different classes of RP phases. To make basic statistical comparisons, the average value of the column coefficients for each category of RP phases are shown in Table 5. As indicated by the regression results, all of the HC-based phases are well fit by the HSM model.

*3.6.3.1. Hydrophobicity.* The overall hydrophobicity of a stationary phase is largely a function of the total surface area of the basic silica gel, the bonding density of the stationary phase, and the nature of the stationary phase itself [48]. These physical and chemical differences can be measured by the H term. As shown in Fig. 11a, the hydrophobicity follows the order: cyano < HC–OH ~ phenyl < HC–COOH ~ fluoro < polar embedded < HC–T ~ –$SO_3$–HC–$C_8$ ~ HC–$C_{8,\ Hi-Sn}$ < HC–$C_{8,\ Z-Sn}$ ~ B–$C_8$ < polar endcapped $C_{18}$ ~ B–$C_{18}$.

As expected the conventional B–$C_{18}$ type phases showed the highest hydrophobicity among all phases considered. Hydrophobicity decreases upon decreasing the chain length as clearly shown by comparing the average $C_{18}$ phase ($H$ = 0.97) vs. the average $C_8$ phase ($H$ = 0.83). Comparing the H of the three reversed HC phases in Table 5, the first generation HC–$C_{8,\ Z-Sn}$ showed a hydrophobicity ($H$ = 0.81) almost identical to the average conventional $C_8$ phase (B–$C_8$). Changing the base silica, Friedel–Crafts catalyst and reaction reagents to produce HC–$C_{8,\ Hi-Sn}$ and HC–T resulted in only a small but real decrease in hydrophobicity to $H$ = 0.75 and 0.72, respectively.

For HC-phases with polar or ionic functionalities, there is no significant difference in H between the HC–$C_{8,\ Hi-Sn}$ phase ($H$ = 0.75) and the strong cation exchange –$SO_3$–HC–$C_8$ phase ($H$ = 0.73). In contrast, the weak cation exchange HC–COOH phase ($H$ = 0.62) and the polar HC–OH phase ($H$ = 0.59) showed substantially reduced hydrophobicity. This agrees well with the order of hydrophobicity measured by the alkylphenone homolog solutes (Section 3.6.2). In fact, the new HC–OH phase exhibits lower hydrophobicity than do the majority of polar-embedded, fluoro and phenyl phases investigated. Previous work [49–51] suggested that the impact of polar groups on hydrophobicity is largely determined by whether the group is embedded or used to end-cap the column. The presence of polar groups inserted (embedded) within the alkyl ligands can make the polar embedded phase substantial more "hydrophilic" (i.e. $H$ = 0.68), while the presence of a polar group as an endcapping agent does not seem to influence the overall hydrophobicity (i.e. $H$ = 0.94.). The 25% decreases in H of HC–OH phase vs. HC–$C_8$ indicate that the hydroxyl groups are likely embedded within the polymer network resulting in a significant reduction in the hydrophobic nature of the hyper-crosslinked platform. In consequence, the average retention of the 16 solutes on the HC–OH phase is about 40% less than that of the HC–$C_{8,\ Hi-Sn}$ phases (Table 6). However, the HC–OH phase is more hydrophobic than are cyano phases, which were previously pointed to as the least hydrophobic reversed phase material [29,52].

*3.6.3.2. Steric resistance.* The $S^*$ coefficient measures a phase's steric resistance to the penetration of bulky solutes into the stationary phase [29]. Similar to the H coefficient, this is largely determined by stationary phase's surface characteristics such as the bonding density, chain length and the presence of the functional groups [29]. It is very important to understand that all HSM coefficients other than the H coefficient are defined as phase properties relative to a "typical" type-B alkyl silica phase. Thus if a phase has a parameter close to zero it means that it behaves in this regard just as does the "typical" phase [29]. Consequently both the conventional $C_8$ and $C_{18}$ phases showed average $S^*$ values close to zero, as shown in Fig. 11b.

It is most interesting to note that the $S^*$ coefficient is clearly negative and large in magnitude on all HC-based phases. In fact, even when we compared the $S^*$ values for over 400 reversed phases reported by Snyder [53], the HC phases showed the most negative value of all phases made with a wide variety of surface chemistries, suggesting that the two solutes (i.e. trans- and cis-chalcone), which are the major determinants of $S^*$, are much more strongly retained on the HC phases than on conventional RPLC phases. The potential causes of the stronger retention of these two solutes on our HC phases are the rather low surface density of $C_8$ groups on the HC–$C_8$ phase ($1.0 \pm 0.1$ μmol/m$^2$) or even the total absence of a long alkyl chain on the HC–OH phase as compared to the typical 2.0–3.5 μmol/m$^2$ of conventional alkylsilica phases.

In addition, we also note that the two $\sigma$ marker compounds are highly aromatic. Our HC phases are also highly aromatic. It is possible that strong π–π interactions might also contribute significantly to the strong retention of the two solutes and consequently lead to an apparent highly negative $S^*$. Such a hypothesis is supported by the negative $S^*$ measured on the cyano and phenyl phases. Previously, Snyder and coworkers pointed out the importance of such interactions on these two types of phases [43,44] and introduced additional solute and phase parameters to deal with them. In the absence of such parameters we believe that π interactions "show up" in the $S^*$ parameter leading to the negative values of the two phases when compared to the conventional alkylsilica phases.

*3.6.3.3. H-bond acidity.* The A coefficient measures the stationary phase H-bond acidity. This is closely associated with the number and accessibility of residual silanol groups on the surface of the silica. As clearly shown in Fig. 11c, the A values are higher for all the

**Table 5**
Comparison of HSM coefficients on HC–OH phase versus several types of commercial stationary phases.[a]

| Stationary phases | Column coefficients | | | | | | | |
|---|---|---|---|---|---|---|---|---|
| | $H$ | $S^*$ | $A$ | $B$ | $C_{-2.8}$ | log $k'_{EB}$ | SE | $r^2$ |
| HC–OH | 0.59 ± 0.03 | −0.22 ± 0.04 | 0.03 ± 0.07 | 0.09 ± 0.03 | 0.19 ± 0.05 | 0.38 ± 0.02 | 0.992 | 0.04 |
| HC–COOH | 0.62 ± 0.03 | −0.28 ± 0.03 | 0.08 ± 0.06 | 0.07 ± 0.02 | 0.38 ± 0.04 | 0.40 ± 0.02 | 0.994 | 0.03 |
| –$SO_3$–HC–$C_8$ | 0.73 ± 0.03 | −0.39 ± 0.05 | 0.21 ± 0.09 | 0.03 ± 0.04 | 2.59 ± 0.07 | 0.53 ± 0.04 | 0.995 | 0.06 |
| HC–$C_{8,\ Hi–Sn}$ | 0.75 ± 0.02 | −0.27 ± 0.03 | 0.13 ± 0.05 | 0.04 ± 0.02 | 0.24 ± 0.03 | 0.69 ± 0.02 | 0.997 | 0.03 |
| HC–$C_{8,\ Z–Sn}$ | 0.81 ± 0.02 | −0.28 ± 0.02 | 0.28 ± 0.03 | 0.02 ± 0.01 | 0.26 ± 0.02 | 0.46 ± 0.01 | 0.999 | 0.02 |
| HC–T | 0.72 ± 0.02 | −0.22 ± 0.02 | 0.38 ± 0.03 | −0.02 ± 0.01 | 0.44 ± 0.02 | 0.20 ± 0.01 | 0.998 | 0.02 |
| Average of cyano[b] | 0.41 ± 0.03 | −0.11 ± 0.01 | −0.58 ± 0.14 | −0.01 ± 0.01 | 0.01 ± 0.17 | 0.16 ± 0.19 | N/A | N/A |
| Average of fluorophenyl[b] | 0.63 ± 010 | 0.14 ± 0.03 | −0.26 ± 0.07 | 0.01 ± 0.04 | 0.55 ± 0.39 | 0.59 ± 0.23 | N/A | N/A |
| Average of phenyl[b] | 0.60 ± 0.07 | −0.16 ± 0.04 | −0.23 ± 0.17 | 0.02 ± 0.02 | 0.16 ± 0.10 | 0.42 ± 0.11 | N/A | N/A |
| Average of polar-embedded[b] | 0.68 ± 0.12 | 0.00 ± 0.05 | −0.54 ± 0.42 | 0.17 ± 0.10 | −0.65 ± 0.29 | 0.66 ± 0.20 | N/A | N/A |
| Average of polar-endcapped[b] | 0.94 ± 0.09 | −0.02 ± 0.01 | −0.01 ± 0.26 | 0.01 ± 0.04 | −0.14 ± 0.15 | 0.92 ± 0.13 | N/A | N/A |
| Average of type B $C_8$[c] | 0.83 ± 0.09 | −0.01 ± 0.04 | −0.16 ± 0.13 | 0.02 ± 0.02 | 0.02 ± 0.20 | 0.69 ± 0.22 | N/A | N/A |
| Average of type B $C_{18}$[d] | 0.97 ± 0.09 | −0.00 ± 0.05 | −0.02 ± 0.16 | −0.02 ± 0.13 | 0.07 ± 0.32 | 0.89 ± 0.21 | N/A | N/A |

[a] The chromatographic conditions are the same as in Fig. 11.
[b] The average column coefficients for different commercial phases were obtained from Ref. [29].
[c] The average column coefficients for type B $C_8$ phases were calculated based upon the 38 commercial type B $C_8$ phases.
[d] The average column coefficients for type B $C_{18}$ were calculated based upon the 108 commercial type B $C_{18}$ phases.

**Table 6**
Performance comparison of Snyder's solutes on HC–OH vs. HC–$C_{8,\ Hi–Sn}$ phase in phosphate buffer.

| Solutes | HC–$C_{8,\ Hi–Sn}$ in 50/50 ACN/$H_2O$[a] | | HC–OH in 50/50 ACN/$H_2O$[a] | | HC–OH/HC–$C_{8,\ Hi–Sn}$[a] | |
|---|---|---|---|---|---|---|
| | $k'$ | $N$ | $k'$ | $N$ | $k'$ ratio[b] | $N$ ratio[b] |
| Acetophenone | 1.59 | 4540 | 0.97 | 4740 | 0.61 | 1.04 |
| Toluene | 3.43 | 4540 | 1.81 | 4770 | 0.53 | 1.05 |
| Ethylbenzene | 4.89 | 4470 | 2.41 | 4940 | 0.49 | 1.11 |
| 4-Nitrophenol | 1.07 | 4210 | 0.79 | 4595 | 0.74 | 1.09 |
| 5-Phenylpentanol | 2.44 | 4420 | 1.50 | 4680 | 0.61 | 1.06 |
| 5,5-Diphenylhydantoin | 1.15 | 3490 | 0.90 | 3860 | 0.78 | 1.11 |
| Benzonitrile | 1.75 | 4600 | 1.06 | 4900 | 0.61 | 1.07 |
| Anisole | 2.42 | 4705 | 1.37 | 5100 | 0.57 | 1.08 |
| N,N-Dimethylacetamide | 0.27 | 2770 | 0.22 | 3470 | 0.81 | 1.25 |
| N,N-Diethylacetamide | 0.54 | 3310 | 0.40 | 3975 | 0.74 | 1.20 |
| 4-n-Butylbenzoic acid | 3.23 | 3825 | 1.96 | 4740 | 0.61 | 1.24 |
| Mefenamic acid | 7.80 | 4175 | 4.25 | 4425 | 0.54 | 1.06 |
| Nortriptyline | 1.10 | 2690 | 0.82 | 3380 | 0.75 | 1.26 |
| Amitriptyline | 1.38 | 2550 | 0.96 | 3350 | 0.70 | 1.31 |
| cis-Chalcone | 7.65 | 4615 | 3.63 | 5275 | 0.47 | 1.14 |
| trans-Chalcone | 10.04 | 4245 | 4.58 | 5370 | 0.46 | 1.27 |
| Average of 16 solutes | | | | | 0.63 | 1.15 |

[a] All chromatographic conditions are the same as in Fig. 11.
[b] Retention and plate count of each solute on the HC–OH phase are normalized by that of the HC–$C_{8,\ Hi–Sn}$ phase.

HC phases compared to the averages of the other types of reversed phases, and are among the highest 10% of all the RPLC columns studied. As previously reported [9–11,14,15], the strong H-bond acidity is primarily caused by the large number of active hydrogen bond donors released upon hydrolyzing the siloxane bonds on the surface of the HC platform during the post-synthesis hot acid washing process. Among the HC phases, the two phases HC–T ($A$ = 0.38) and HC–$C_{8,\ Z–Sn}$ ($A$ = 0.28) made on Zorbax showed higher $A$ values, presumably due to the higher intrinsic activity of this type of silica. The $A$ coefficient decreases a bit upon using higher purity silica, optimizing the Friedel–Crafts catalyst and reaction conditions (e.g., second generation of HC–$C_{8,\ Hi–Sn}$ ($A$ = 0.13)). A further reduction in $A$ is observed on the HC–OH phase, which exhibits a H-bond acidity close to that of a conventional $C_{18}$ phase, suggesting that the presence of these polar groups effectively reduces access to the silanol groups. The basic polar groups may interact with the active H-bond

**Table 7**
Performance comparison of basic solutes on HC–OH vs. SB $C_{18}$ phase in 0.1% formic acid.[a]

| Solutes | SB $C_{18}$ in 24/76 ACN/water | | HC–OH in 18/82 ACN/water | | HC–OH/SB $C_{18}$ | |
|---|---|---|---|---|---|---|
| | $k'$ | $N$ | $k'$ | $N$ | $k'$ ratio[b] | $N$ ratio[b] |
| Acetophenone | 6.99 | 4700 | 5.76 | 5150 | 0.82 | 1.09 |
| Alprenolol | 5.92 | 2570 | 5.28 | 3960 | 0.89 | 1.54 |
| Nortriptyline | 25.17 | 3600 | 29.85 | 4100 | 1.19 | 1.14 |
| Amitriptyline | 28.32 | 3260 | 35.77 | 4040 | 1.26 | 1.24 |
| Average of three basic solutes | | 3140 | | 4030 | | 1.31 |

[a] Chromatographic conditions: HC–OH column and SB $C_{18}$ phases both have the dimension of 5.0 cm × 0.46 cm, particle diameter = 5 μm. Mobile phases: SB $C_{18}$: 24/76 (v/v) ACN/water with 0.1% formic acid; HC–OH: 18/82 (v/v) ACN/water with 0.1% formic acid; $T$ = 40 °C, $F$ = 1.0 mL/min, λ = 210 nm. 0.2–0.4 nmol of basic analytes were injected into both phases.
[b] Retention and plate count of each solute on the HC–OH phase are normalized by that of the SB $C_{18}$ phase.

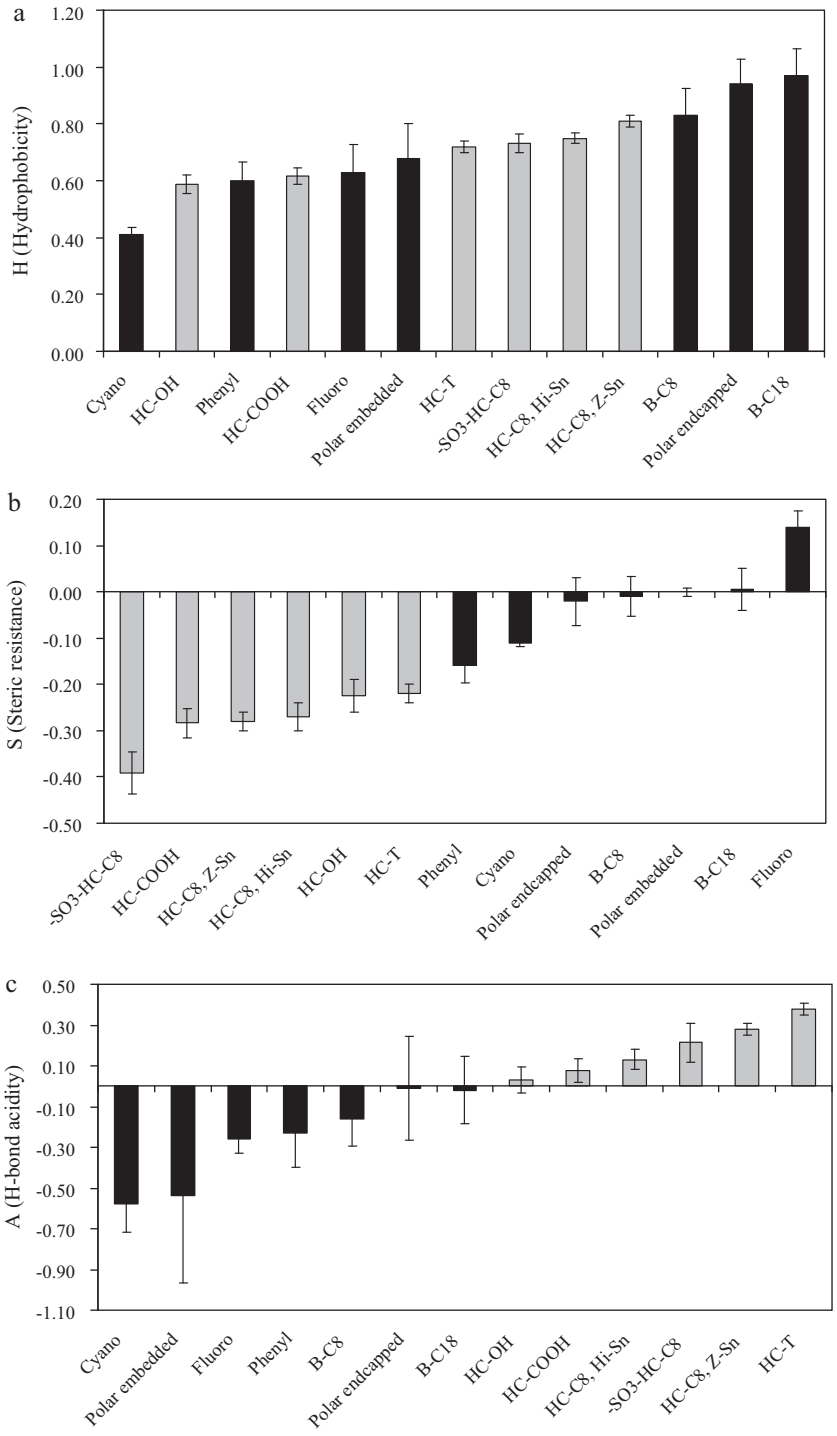


**Fig. 11.** The column selectivity parameters of different phases measured by HSM method. Chromatographic conditions: 50/50 ACN/60 mM phosphate buffer (pH 2.8), $T = 35\,^{\circ}C$, $F = 1.0$ mL/min. The squared correlation coefficients and the standard errors of the regression of Eq. (2) indicate good fits for all five phase. The data for HC–$C_{8,\,Z\text{-}Sn}$ and HC–T were obtained from Ref. [15]; the data for HC–$C_{8,\,Hi\text{-}Sn}$, –$SO_3$–HC–$C_8$, and HC–COOH were obtained from Ref. [14]. The data for cyano, phenyl, polar embedded, polar endcapped, fluoro phases were obtained from Ref. [29]. The data on alkylsilica phases were calculated based upon 108 type-B $C_{18}$ phases and 38 type-B $C_8$ phases.

donors (i.e., silanol) to reduce their acidity, with a net decrease in the number of accessible acidic silanol groups available for solutes. This is consistent with the studies of O'Gara et al. [49] and McCalley et al. [50], where they also found significant reduced retention of various H-bond active probes on polar-embedded phases compared to conventionally bonded $C_{18}$ phases.

*3.6.3.4. H-bond basicity.* The *B* term, H-bond basicity, reflects the ability of a stationary phase to interact with hydrogen-donor solutes, and was determined by injecting a series of carboxylic acids. The origin of the column hydrogen-bond basicity is not fully understood. One hypothesis is that water sorbs into the stationary phase and acts as the source of the hydrogen-bond acceptor [29].

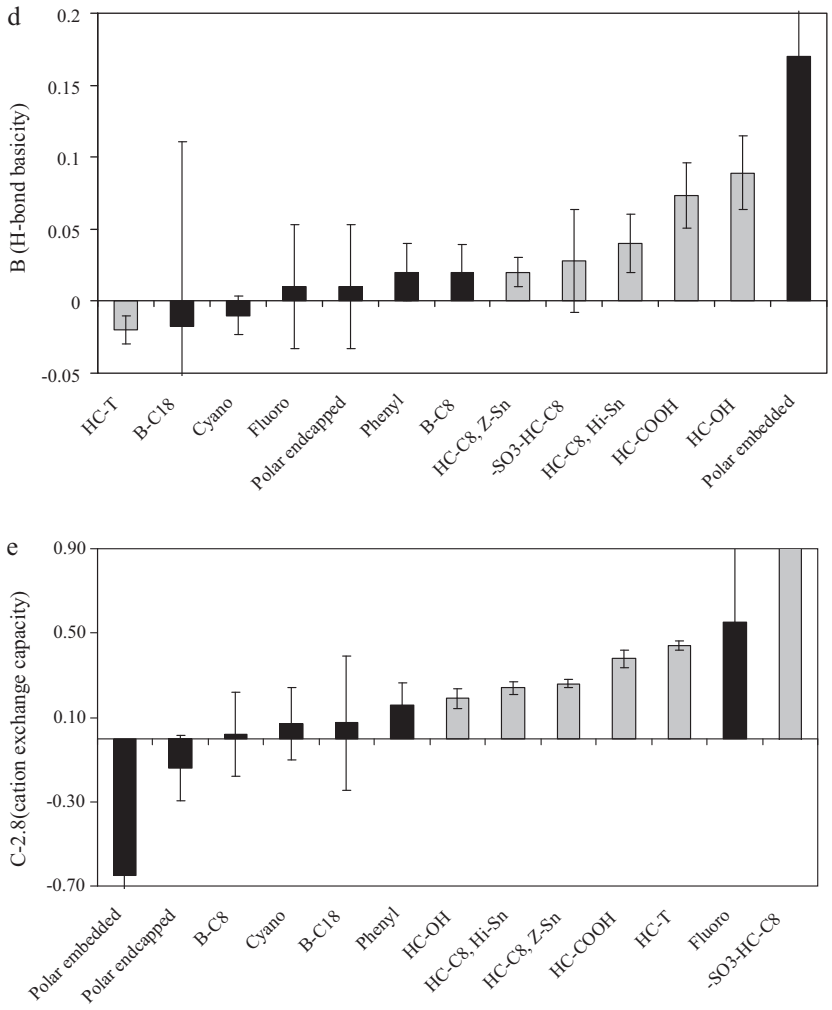


**Fig. 11.** (*Continued*).

This hypothesis correlates very well with the B of the HC phases: HC–OH > HC–COOH > HC–$C_{8,\ Z\text{-}Sn}$ ~ –$SO_3$–HC–$C_8$ ~ HC–$C_{8,\ Hi\text{-}Sn}$ > HC–T, that the *B* value appears to increase with decreasing column hydrophobicity *H*, indicating the column hydrogen-bond basicity is enhanced with higher concentration of water in the stationary phase. In addition, the benzylic hydroxyl groups on the HC–OH phase can also interact with active H-bond donor solutes through H-bonding. This can further increase the retention of hydrogen bond acids. Snyder et al. [29] similarly noted pronounced retention of acidic compounds on Embedded Polar Group (EPG) phases. This too was attributed to the presence of basic polar embedded groups as additional point of H-bonding activity.

*3.6.3.5. Cation exchange capacity*. The *C*(2.8) term indicates the extent of ion exchange interactions with basic analytes under conditions in which the majority of the residual silanol groups are protonated. The cation exchange capability at pH 2.8 follows the order: polar embedded < polar endcapped < B–$C_8$ ~ cyano ~ B–$C_{18}$ < phenyl ~ –OH < HC–$C_{8,\ Hi\text{-}Sn}$ ~ HC–$C_{8,\ Z\text{-}Sn}$ < HC–COOH < HC–T < fluoro < –$SO_3$–HC–$C_8$.

As expected, radically different cation exchange interactions were observed for the HC phases derivatized with different functionalities. In particular, the strong cation exchange phase –$SO_3$–HC–$C_8$ had extraordinarily high cation exchange character ($C_{-SO_3-HC-C_8} = 2.59$) due to the presence of 0.11 μmol/$m^2$ of sulfonate groups. This is followed by the HC–T ($C_{HC-T} = 0.44$) phase which is based on a more active silica substrate (Zorbax), and then the weak cation exchange phase HC–COOH ($C_{HC-COOH} = 0.38$) where the ionization of carboxylic acid groups is still highly suppressed at pH 2.8 but is greatly enhanced at pH 7.0 upon ionization of the carboxylic acid group [14]. The C coefficients of the two HC–$C_8$ phases are very similar, both of which are slightly higher than average type B $C_8$. We believe this results from: (a) the large number of surface silanol groups released by the hot acid treatment; (b) the HC phases are deliberately not endcapped. The decision was made because they are designed to be used in strongly acid media and thus any endcapping would be rapidly lost. The cation exchange capacity is clearly reduced upon introduction of the polar benzylic hydroxyl groups on the HC–OH phase, which exhibits a $C_{-2.8}$ value close to the average of the phenyl phases. This is consistent with the reduced silanol activity as indicated by the lower A (H-bond acidity) value of the HC–OH phase versus the HC–$C_{8,\ Hi\text{-}Sn}$ phase. This also confirms the "shielding" of the silanols by the basic polar groups on the new phase. This might well contribute to the improved peak shape of basic drugs as discussed in the next section.

*3.6.4. Efficiency characterization by basic analytes*

The retention and observed plate counts of the 16 HSM solutes were determined on reversed HC–$C_{8,\ Hi\text{-}Sn}$ and HC–OH phase (Table 6). With the same eluent, the HC–OH phase is less retentive than the HC–$C_{8,\ Hi\text{-}Sn}$; the average retention factors are reduced by 38% on the new phase as compared to the HC–$C_{8,\ Hi\text{-}Sn}$ phase,

consistent with the above discussion. More importantly, the solutes in general showed ~15% higher plate counts on the HC–OH phase vs. the HC–$C_{8,\ Hi–Sn}$ phase. This is especially pronounced for the two basic probes and the hydrogen-bond markers, with the plate counts of amitriptyline and nortriptyline increased by 31% and 26%, and that of dimethylacetamide and diethylacetamide increased by 25% and 20%, respectively. Such improved efficiencies can be attributed to the suppression of the silanol acidity on the new phase, which we believe is the main reason for the bad peak shapes and poor plate counts specifically for cationic analytes [54–56]. This lower silanol activity vs. conventional alkylsilica phases is consistent with several published studies [49,51,57], wherein superior separation efficiencies of EPG phases are observed for basic analytes when compared to the non-EPG analogs. The "shielding" effect of silanols on the HC–OH phase made it possible to analyze the basic solutes even at low ionic strength and/or with weakly ion pairing reagents. For example, three prototypical basic solutes were separated on the HC–OH phase in 0.1% formic acid and compared with a commercial SB $C_{18}$ phase (Table 7). The volume fractions of acetonitrile in the mobile phase were adjusted appropriately to obtain similar retention on both phases. Clearly the observed plate counts of the basic analytes are significantly higher on the HC–OH phase than on the SB $C_{18}$ phase, with an average 30% increase in plate counts obtained on this new highly hydrophilic hypercrosslinked phase.

## 4. Summary

We have developed a family of RPLC stationary phases based on novel hyper-crosslinked polymer-coated silica particles. These phases were designed to have three of the most important characteristics for a new stationary phase: *stability*, *efficiency* and *novel selectivity*. The main conclusions are as follows:

(1) Both the SEM images and the accelerated acid aging test of HC phases show that an extensively connected network polymer is formed on the silica surface. Hence these silica-based HC phases show significantly enhanced acid and thermal stability compared to the most acid stable, commercial RPLC phases.
(2) ISEC and van Deemter flow curve studies have shown that there is little or no pore blockage on the HC platform even after the extensive "orthogonal polymerization". The excellent mass transfer properties of monomeric bonded phases were preserved on these HC materials and none of the adverse kinetic effects of depositing a polymer have been observed. Thus the separation efficiency for both neutral and small basic analytes on this type of material was comparable if not better than a number of very high quality mono-functional conventional phases.
(3) Based on the results obtained with the Snyder–Dolan HSM for evaluating phase selectivity, each of the HC phases showed some distinctive retention mechanism due to the different crosslinking conditions as well as the final derivatization steps. Such unique retention mechanisms led to the different selectivities of the HC phases which distinguish them not just from conventional RP phases but also from each other. Thus the new phases offer different degrees of hydrophobicity and cation exchange capacity which can be used to achieve the separation of a wide range of solutes.

Given their superb acid stability, excellent chromatographic efficiency and novel selectivity, we believe the HC phases will be useful for ultra fast high temperature chromatography or as the separation media in high temperature fast 2DLC. The excellent peak shapes indicate that they should be useful for LC–MS analysis of bases in acidic media.

## Acknowledgements

We thank the National Institute of Health for the financial support (Grant GM54585). Also Mac-Mod Analytical (Chadds Ford, PA) for donation of the HiChrom silica and ACE $C_{18}$ stationary phase, Agilent Technologies Inc. (Wilmington, DE) is thanked for the donation of Zorbax silica and the SB $C_{18}$ phase, and Varian Inc. (Palo Alto, CA) for the donation of Inertsil ODS 3 columns.

## References

[1] A. Berthod, J. Chromatogr. 549 (1991) 1.
[2] M.R. Buchmeiser, J. Chromatogr. A 918 (2001) 233.
[3] J. Nawrocki, J. Chromatogr. A 779 (1997) 29.
[4] J. Nawrocki, B. Buszewski, J. Chromatogr. 449 (1988) 1.
[5] L.C. Sander, S.A. Wise, CRC Critical Reviews in Analytical Chemistry, CRC Press, Boca Raton, 1987, p. 299.
[6] D.J. Anderson, Anal. Chem. 67 (1995) 475R.
[7] J.L. Glajch, J.J. Kirkland, J. Koehler, J. Chromatogr. 384 (1987) 81.
[8] J.J. Kirkland, J.L. Glajch, R.D. Farlee, Anal. Chem. 61 (1989) 2.
[9] H. Luo, L.J. Ma, Y. Zhang, P.W. Carr, J. Chromatogr. A 1182 (2008) 41.
[10] L.J. Ma, H. Luo, J. Dai, P.W. Carr, J. Chromatogr. A 1114 (2006) 21.
[11] B.C. Trammell, L. Ma, H. Luo, M.A. Hillmyer, P.W. Carr, J. Am. Chem. Soc. 125 (2003) 10504.
[12] B.C. Trammell, L.J. Ma, H. Luo, M.A. Hillmyer, P.W. Carr, J. Chromatogr. A 1060 (2004) 61.
[13] B.C. Trammell, L.J. Ma, H. Luo, D.H. Jin, M.A. Hillmyer, P.W. Carr, Anal. Chem. 74 (2002) 4634.
[14] Y. Zhang, P.W. Carr, J. Chromatogr. A 1218 (2011) 763.
[15] Y. Zhang, Y. Huang, P.W. Carr, J. Sep. Sci. 34 (2011) 1407.
[16] J.D. Thompson, P.W. Carr, Anal. Chem. 74 (2002) 4150.
[17] B.W. Yan, J.H. Zhao, J.S. Brown, J. Blackwell, P.W. Carr, Anal. Chem. 72 (2000) 1253.
[18] D.R. Stoll, X.P. Li, X.O. Wang, P.W. Carr, S.E.G. Porter, S.C. Rutan, J. Chromatogr. A 1168 (2007) 3.
[19] X.L. Wang, D.R. Stoll, P.W. Carr, P.J. Schoenmakers, J. Chromatogr. A 1125 (2006) 177.
[20] M. Hanson, B. Eray, K. Unger, A.V. Neimark, J. Schmid, K. Albert, E. Bayer, Chromatographia 35 (1993) 403.
[21] M. Hanson, K.K. Unger, Trac-Trend Anal. Chem. 11 (1992) 368.
[22] J. Li, P.W. Carr, Anal. Chem. 69 (1997) 2193.
[23] J. Li, D.H. Reeder, A.V. McCormick, P.W. Carr, J. Chromatogr. A 791 (1997) 45.
[24] H. Engelhardt, G. Ahr, Chromatographia 14 (1981) 227.
[25] U.D. Neue, in: R.A. Meyers (Ed.), Encyclopedia of Analytical Chemistry, John Wiley and Sons, New York, 2000.
[26] V.A. Davankov, C.S. Sychov, M.M. Ilyin, K.O. Sochilina, J. Chromatogr. A 987 (2003) 67.
[27] M.J. Wirth, R.W.P. Fairbank, H.O. Fatunmbi, Science 275 (1997) 44.
[28] X.Q. Yang, L.J. Ma, P.W. Carr, J. Chromatogr. A 1079 (2005) 213.
[29] L.R. Snyder, J.W. Dolan, P.W. Carr, J. Chromatogr. A 1060 (2004) 77.
[30] H. Luo, L.J. Ma, C. Paek, P.W. Carr, J. Chromatogr. A 1202 (2008) 8.
[31] D.H. Reeder, J. Li, P.W. Carr, M.C. Flickinger, A.V. McCormick, J. Chromatogr. A 760 (1997) 71.
[32] J. Nawrocki, Chromatographia 31 (1991) 177.
[33] J. Nawrocki, Chromatographia 31 (1991) 193.
[34] J. Dai, S.D. Mendonsa, M.T. Bowser, C.A. Lucy, P.W. Carr, J. Chromatogr. A 1069 (2005) 225.
[35] X.Q. Yang, J. Dai, P.W. Carr, J. Chromatogr. A 996 (2003) 13.
[36] L. Ma, Acid stable hyper crosslinked stationary phases for the reversed phase high performance liquid chromatographic separation of basic and biological analytes, Department of Chemistry, University of Minnesota, Minneapolis, 2005.
[37] H. Luo, A silica-based hydrophobic cation exchange phase for water soluble pharmaceuticals and bioactive analytes, Department of Chemistry, University of Minnesota, Minneapolis, 2006.
[38] N.E. Oro, C.A. Lucy, J. Chromatogr. A 1217 (2010) 6178.
[39] L.R. Snyder, J.L. Glajch, J.J. Kirkland, Practical HPLC Method Development, Wiley-Interscience, New York, 1996.
[40] J.J. Gilroy, J.W. Dolan, L.R. Snyder, J. Chromatogr. A 1000 (2003) 757.
[41] J.J. Gilroy, J.W. Dolan, P.W. Carr, L.R. Snyder, J. Chromatogr. A 1026 (2004) 77.
[42] N.S. Wilson, J. Gilroy, J.W. Dolan, L.R. Snyder, J. Chromatogr. A 1026 (2004) 91.
[43] D.H. Marchand, K. Croes, J.W. Dolan, L.R. Snyder, J. Chromatogr. A 1062 (2005) 57.
[44] D.H. Marchand, K. Croes, J.W. Dolan, L.R. Snyder, R.A. Henry, K.M.R. Kallury, S. Waite, P.W. Carr, J. Chromatogr. A 1062 (2005) 65.

[45] N.S. Wilson, M.D. Nelson, J.W. Dolan, L.R. Snyder, R.G. Wolcott, P.W. Carr, J. Chromatogr. A 961 (2002) 171.
[46] N.S. Wilson, M.D. Nelson, J.W. Dolan, L.R. Snyder, P.W. Carr, J. Chromatogr. A 961 (2002) 195.
[47] N.S. Wilson, J.W. Dolan, L.R. Snyder, P.W. Carr, L.C. Sander, J. Chromatogr. A 961 (2002) 217.
[48] K. Kimata, K. Iwaguchi, S. Onishi, K. Jinno, R. Eksteen, K. Hosoya, M. Araki, N. Tanaka, J. Chromatogr. Sci. 27 (1989) 721.
[49] J.E. O'Gara, B.A. Alden, T.H. Walter, J.S. Petersen, C.L. Niederlaender, U.D. Neue, Anal. Chem. 67 (1995) 3809.
[50] D.V. McCalley, J. Chromatogr. A 844 (1999) 23.
[51] J. Layne, J. Chromatogr. A 957 (2002) 149.
[52] U.D. Neue, J.E. O'Gara, A. Mendez, J. Chromatogr. A 1127 (2006) 161.
[53] L.R. Snyder, Column Match Database (personal communication with Dr. L.R. Snyder).
[54] S.M.C. Buckenmaier, D.V. McCalley, M.R. Euerby, Anal. Chem. 74 (2002) 4672.
[55] J.E. Eble, R.L. Grob, P.E. Antle, L.R. Snyder, J. Chromatogr. 384 (1987) 45.
[56] D.V. McCalley, J. Chromatogr. A 793 (1998) 31.
[57] E. Cruz, M.R. Euerby, C.M. Johnson, C.A. Hackett, Chromatographia 44 (1997) 151.